SARS-CoV-2 spike-specific memory B cells express markers of durable immunity after non-severe COVID-19 but not after severe disease — Source link ↗

Raphael A. Reyes, Kathleen N. Clarke, S. Jake Gonzales, Angelene M. Cantwell ...+6 more authors

Institutions: University of Texas Health Science Center at San Antonio

Related papers:

- Switched and unswitched memory B cells detected during SARS-CoV-2 convalescence correlate with limited symptom duration.

- SARS-CoV-2-specific T cell memory is long-lasting in the majority of convalsecent COVID-19 individuals

- Immune memory in convalescent patients with asymptomatic or mild COVID-19

- Immunological memory to SARS-CoV-2 assessed for greater than six months after infection

- Longitudinal Analysis of Human Memory T-Cell Response According to the Severity of Illness up to 8 Months After Severe Acute Respiratory Syndrome Coronavirus 2 Infection.

Share this paper: f 𝕏 in ✉

View more about this paper here: https://typeset.io/papers/sars-cov-2-spike-specific-memory-b-cells-express-markers-of-47gc08fi1z

1   **SARS-CoV-2 spike-specific memory B cells express markers of durable immunity after**

2   **non-severe COVID-19 but not after severe disease**

3

4   Raphael A. Reyes[1], Kathleen Clarke[1], S. Jake Gonzales[1], Angelene M. Cantwell[1], Rolando

5   Garza[1], Gabriel Catano[2], Robin E. Tragus[2], Thomas F. Patterson[2], Sebastiaan Bol[1], Evelien M.

6   Bunnik[1]*

7

8   [1] Department of Microbiology, Immunology and Molecular Genetics, Long School of Medicine,

9   The University of Texas Health Science Center at San Antonio, San Antonio, TX, USA

10 [2] Department of Medicine, Division of Infectious Diseases, The University of Texas Health

11 Science Center at San Antonio, University Health System, San Antonio, TX, USA

12 [3] The South Texas Veterans Health Care System, San Antonio, TX, USA

13

14 *Correspondence

15 Evelien M. Bunnik, Ph.D.

16 bunnik@uthscsa.edu

17 7703 Floyd Curl Drive

18 San Antonio, TX 78229

19 United States of America

20 +1 210-450-8146

21

22 **Conflict of interest statement:** The authors have declared that no conflict of interest exists.

23 **Keywords:** T-bet; FcRL5; adaptive immunity; humoral immune response; IgM; IgG

24   **ABSTRACT**

25   SARS-CoV-2 infection elicits a robust B cell response, resulting in the generation of long-lived

26   plasma cells and memory B cells. Here, we aimed to determine the effect of COVID-19 severity

27   on the memory B cell response and characterize changes in the memory B cell compartment

28   between recovery and five months post-symptom onset. Using high-parameter spectral flow

29   cytometry, we analyzed the phenotype of memory B cells with reactivity against the SARS-CoV-

30   2 spike protein or the spike receptor binding domain (RBD) in recovered individuals who had

31   been hospitalized with non-severe (n=8) or severe (n=5) COVID-19. One month after symptom

32   onset, a substantial proportion of spike-specific IgG$^+$ B cells showed an activated phenotype. In

33   individuals who experienced non-severe disease, spike-specific IgG$^+$ B cells showed increased

34   expression of markers associated with durable B cell memory, including T-bet, FcRL5, and

35   CD11c, which was not observed after severe disease. Five months post-symptom onset, the

36   majority of spike-specific memory B cells had a resting phenotype and the percentage of spike-

37   specific T-bet$^+$ IgG$^+$ memory B cells decreased to baseline levels. Collectively, our results

38   suggest that the memory B cell response elicited during non-severe COVID-19 may be of higher

39   quality than the response after severe disease.

40 **INTRODUCTION**

41 Severe acute respiratory syndrome coronavirus 2 (SARS-CoV-2) is responsible for the global

42 coronavirus disease 2019 (COVID-19) pandemic resulting in more than 4 million deaths

43 reported worldwide as of September 2021 (1). Highly efficacious vaccines have limited SARS-

44 CoV-2 transmission and significantly reduced morbidity and mortality in regions of the world with

45 access to these vaccines. However, the majority of the world's population lives in areas with low

46 vaccination rates and remain at higher risk of SARS-CoV-2 infection and COVID-19. Both

47 vaccination and natural infection elicit immunological protection against SARS-CoV-2 (re-

48)infection. Although mRNA vaccination elicits higher antibody titers and more diverse antibody

49 responses against the SARS-CoV-2 spike protein than natural infection (2, 3), results from the

50 first longitudinal studies in unvaccinated individuals with prior COVID-19 suggest that naturally

51 acquired immune responses are maintained for at least a year after infection and that these

52 responses protect from subsequent re-infection (4-11). Because many people remain

53 unvaccinated, it will be important to understand the immune response elicited by natural

54 infection and whether the durability of naturally acquired immunity is influenced by the severity

55 of disease.

56

57 Although SARS-CoV-2 infection elicits robust responses in both the T cell and B cell arms of the

58 adaptive immune system (12, 13), the majority of research efforts have focused on B cell and

59 antibody responses, which are thought to be critical for the control of infection and protection

60 against re-infection. Humoral immune responses against pathogens consist of multiple

61 components. The early B cell response is dominated by short-lived antibody-secreting cells,

62 called plasmablasts. Simultaneously, other B cell populations undergo selection for high affinity

63 antigen-binding in germinal centers of the secondary lymphoid organs, and can differentiate into

64 long-lived, antibody-secreting plasma cells that migrate to the bone marrow or into memory B

65 cells that remain in the circulation (reviewed in (14)). COVID-19 patients rapidly generate potent

66   neutralizing IgG antibodies against the spike protein (15, 16). Anti-spike antibody titers peak

67   within the first two months post-infection, decline in the subsequent 3 – 4 months, and then

68   plateau at titers higher than those detected in pre-pandemic samples, but are lower than anti-

69   spike antibody titers elicited by vaccination (3, 5, 7, 17). These phases of the anti-spike IgG

70   profile in the circulation are the result of early short-lived plasmablast responses, followed by the

71   secretion of antibodies by longer-lived bone marrow plasma cells (5). In addition, spike-specific

72   IgG$^+$ memory B cells are maintained or even increase in numbers for at least six months to one

73   year following SARS-CoV-2 infection (6-8, 18). Analysis of monoclonal antibodies obtained from

74   these memory B cells revealed continued evolution of the B cell response over time, as

75   evidenced by higher levels of somatic hypermutation, resulting in increased binding affinity and

76   neutralizing capacity (7, 19, 20).

77

78   In recent years, novel subsets of activated B cells and memory B cells have been identified.

79   These novel B cell subsets have mainly been defined by their phenotype, that is, the collection

80   of markers expressed on their cell surface or intracellularly, and are thought to possess either

81   protective or pathogenic functions in the immune response. For example, several subsets of

82   double negative (DN; CD27$^-$ IgD$^-$) B cells have been defined in recent years (21, 22). Type 1

83   double negative cells (DN1 cells), defined as DN cells that express CXCR5 or CD21 and lack

84   CD11c and FcRL5, are transcriptionally similar to class-switched memory B cells and seem to

85   be part of a functional B cell response (21, 23). On the other hand, type 2 DN cells (DN2 cells),

86   defined as CD11c$^+$/FcRL5$^+$ and CXCR5$^-$/CD21$^-$ DN cells, are thought to arise from the activation

87   of naïve B cells outside of the B cell follicle in the lymph node. Type 3 DN cells (DN3 cells),

88   defined as CD11c$^-$/FcRL5$^-$ and CXCR5$^-$/CD21$^-$ DN cells, have also been associated with this

89   extrafollicular response and may be DN2 cell precursors (22, 23). DN2 cells are more abundant

90   in patients with autoimmune disorders, such as systemic lupus erythematosus, and are thought

91   to differentiate into auto-antibody-secreting cells. DN2 cells are also observed in the circulation

92   of patients with severe COVID-19 (22), an observation that has been linked to lack of germinal

93   center formation, presumably leading to an impaired B cell response (24).

94

95   Interestingly, memory B cells (CD27$^+$ IgD$^-$) expressing some of the same markers as DN2 cells,

96   including CD11c and FcRL5, as well as the transcription factor T-bet, have been described as

97   part of normal, functional immune responses (25, 26). Specifically, these cells have been

98   implicated in long-lived B cell memory after tetanus toxoid and influenza virus vaccination (27,

99   28). In recovered COVID-19 patients, memory B cells present 1 – 3 months after symptom

100   onset are also found to express FcRL5 and T-bet, suggesting that these markers may delineate

101   a subset of long-lived memory B cells against SARS-CoV-2 (13, 29). However, it is unclear

102   whether disease severity influences the development of memory B cells that express T-bet or

103   FcRL5, and whether the phenotype of memory B cells changes with the continued evolution of

104   this B cell compartment in the months following SARS-CoV-2 infection. A more detailed analysis

105   of B cell subsets in recovered COVID-19 patients will therefore be needed to acquire insight into

106   the early B cell response and the evolution of memory B cells over time.

107

108   Here, we performed spectral flow cytometry to characterize the phenotype of SARS-CoV-2-

109   specific B cells in unvaccinated patients who recovered from non-severe or severe COVID-19.

110   We focused on two comparative analyses. First, we compared the phenotype of spike-specific B

111   cells between convalescent patients who were hospitalized with non-severe and severe disease

112   to determine whether the B cell response developed differently in these two groups. Second, we

113   compared the phenotype of memory B cells shortly after recovery to that at five months post-

114   symptom onset to analyze the ongoing evolution of the B cell response. The results from this

115   study provide insight into naturally acquired B cell memory against SARS-CoV-2 and a better

116   understanding of the characteristics of durable B cell immunity.

117   **RESULTS**

118   **Study criteria**

119   Study participants (n=16) were enrolled in the Adaptive COVID-19 Treatment Trial (ACTT)-1 or

120   ACTT-2 clinical trials which were designed to evaluate the effect of remdesivir or baricitinib plus

121   remdesivir for the treatment of COVID-19 in hospitalized patients (30, 31). Participants identified

122   predominantly as white (94%) and Hispanic (75%), and all except one individual had one or

123   more comorbidities (**Table S1**). Participants were classified as non-severe (n = 11) or severe (n

124   = 5) COVID-19 cases based on their worst ordinal score for disease severity during hospital

125   stay. In summary, non-severe cases did not require supplemental oxygen (score = 4) or

126   required supplemental oxygen or non-invasive ventilation (score = 5 or 6), while severe cases

127   needed invasive mechanical ventilation (MV) or extracorporeal membrane oxygenation (ECMO)

128   (score = 7). The definition of severe disease was made based on the need for MV or ECMO,

129   because this distinguishes the most critical patients, who are the most likely to develop impaired

130   immune responses (24, 32). Blood was collected after discharge from the hospital (a median of

131   30 days after symptom onset for non-severe cases (n = 8) and 32 days after symptom onset for

132   severe cases (n = 5)) (**Figure 1**). For participants with non-severe disease, additional samples

133   were collected at an earlier time point (a median of 18 days post-symptom onset; n = 9) and at a

134   follow-up visit approximately 5 months post-symptom onset (median, 147 days; n = 7) based on

135   availability and consent. Peripheral blood mononuclear cells (PBMCs) from healthy donors (n =

136   3) collected before the start of the pandemic (2018 or early 2019) were used as negative

137   controls.

138

139   **The proportions of B cell subsets in convalescent patients are similar between non-**

140   **severe and severe COVID-19 cases**

141   Severe COVID-19 is associated with an extrafollicular B cell response characterized by a high

142   percentage of DN2 B cells in the circulation, similar to what is observed in patients with

6

143   autoimmune disorders (21, 22). Previous data suggest that the percentage of DN2 B cells in

144   patients with severe COVID-19 had returned to normal levels approximately 1.5 months after

145   hospital discharge (33). To determine whether COVID-19 severity affects the distribution of B

146   cell subsets shortly after recovery (four to five weeks after symptom onset), we analyzed the

147   relative proportions of B cell subsets individuals who recovered from non-severe (n = 8) or

148   severe (n = 5) disease by spectral flow cytometry using an antibody panel against 19 cell

149   surface and intracellular markers (**Table S2**). B cells were first gated on live, CD19$^+$ CD20$^+$

150   CD38$^{-/lo}$ cells to exclude transitional B cells and antibody-secreting cells, and were subsequently

151   divided into naïve (CD27$^-$ IgD$^+$), unswitched memory (CD27$^+$ IgD$^+$), resting switched memory

152   (CD27$^+$ IgD$^-$ CD21$^+$), activated switched memory (CD27$^+$ IgD$^-$ CD21$^-$) and double negative (DN;

153   CD27$^-$ IgD$^-$) B cells (**Figure 2A**). Apart from a significant increase in the percentage of

154   unswitched memory B cells in individuals who had experienced severe disease compared to

155   those with non-severe COVID-19, no differences in the distribution of these B cell subsets were

156   observed between the two groups of recovered COVID-19 patients (**Figure 2B-C, Figure S1A**).

157   Among DN cells, DN1 (FcRL5$^-$ CXCR5$^+$) B cells were the dominant subset in both groups of

158   recovered COVID-19 patients, and we did not detect significant differences in the frequencies of

159   DN1, DN2 (FcRL5$^+$ CXCR5$^-$), and DN3 (FcRL5$^-$ CXCR5$^-$) B cells between the two groups

160   (**Figure 2D, Figure S1B**). In combination with previous reports (22, 33), these results suggest

161   that expansion of the DN2 B cell population during severe COVID-19 might be transient and that

162   these cells disappear soon after recovery.

163

164   **The percentage of spike-specific and RBD-specific B cells and their isotype distributions**

165   **are similar between non-severe and severe cases**

166   Our flow cytometry panel also included antigen probes to detect B cells reactive with the SARS-

167   CoV-2 spike protein and the spike receptor binding domain (RBD). RBD is the part of the spike

168   protein that interacts with angiotensin-converting enzyme 2, the viral receptor on host cells, and

7

169   is the dominant target of neutralizing antibodies (34). However, the majority of antibodies

170   generated against the spike protein bind to epitopes outside RBD (35). Whereas the RBD

171   sequence is highly specific for SARS-CoV-2 (36), the non-RBD parts of spike, in particular the

172   S2 subunit, share epitopes with other coronaviruses that circulate in the human population (37-

173   39). Evidence for pre-existing memory B cells that are cross-reactive with other coronaviruses

174   has been reported (40). Because pre-existing immunity could affect the development of the

175   immune responses against these two parts of the spike protein, we analyzed B cell responses

176   against RBD and non-RBD spike epitopes separately.

177

178   We constructed spike tetramers in two fluorochrome formats and defined the population of cells

179   staining positive for both tetramers as spike-specific (**Figure 3A**). The spike-specific B cells

180   were then divided into non-RBD-specific and RBD-specific B cells based on reactivity with the

181   RBD tetramer (**Figure 3A**). Non-RBD-specific and RBD-specific B cells were strongly enriched

182   for antigen-experienced B cells (**Figure 3B,** compare to **Figure 2B**), with no statistically

183   significant differences in the proportions of various B cell populations between individuals who

184   recovered from non-severe or severe disease (**Figure 3B, Figure S2**). In addition, reactivity

185   against spike and RBD tetramers among control donor B cells was minimal (**Figure 3A,C**),

186   suggesting that these probes selectively bind to antigen-specific B cells.

187

188   The percentage of spike-specific B cells among antigen-experienced B cell populations

189   (unswitched memory, switched memory, and DN B cells) among all patients ranged from 0.1%

190   to 1.8% (median, 0.6%) (**Figure 3C**). One donor (marked with # in Figure 3C) had only six

191   spike-specific B cells and was therefore not included in subsequent analyses that required

192   further subsetting of these cells. All other donors had between 42 and 450 spike-specific B cells.

193   In line with a previous study (4), a median of 22% of spike-specific B cells were reactive against

194   RBD (**Figure 3D**). Ogega *et al*. recently reported that patients who recovered from severe

8

195   COVID-19 harbored more RBD-specific B cells than COVID-19 patients who never required

196   hospitalization (29). We did not observe a difference in the percentage of RBD-specific cells

197   between individuals who recovered from non-severe and severe disease, potentially because

198   our non-severe group had been hospitalized and suffered from more severe disease than the

199   group with non-severe disease in the Ogega *et al.* study.

200

201   Next, we compared the isotype of class-switched spike-specific B cells between patients who

202   recovered from non-severe and severe COVID-19 by categorizing spike-specific antigen-

203   experienced B cells based on IgM, IgG, or IgA expression. The percentage of IgM$^+$, IgG$^+$, and

204   IgA$^+$ class-switched B cells among spike-specific B cells did not differ significantly between the

205   two patient groups and in both groups, the majority of class-switched spike-specific B cells were

206   IgG$^+$ (**Figure 3E**). We also determined plasma IgM and IgG reactivity to the spike protein and

207   RBD and observed no significant differences in IgM or IgG titers to the spike protein or RBD

208   between convalescent patients who recovered from non-severe or severe disease (**Figure 3F**).

209   Collectively, these results suggest that individuals who recovered from either non-severe or

210   severe COVID-19 have similar immune responses to the SARS-CoV-2 spike protein, in terms of

211   the prevalence of spike-specific B cells and their major phenotype.

212

213   **Non-severe COVID-19 is associated with an increased population of T-bet$^+$ spike-specific**

214   **IgG$^+$ B cells**

215   To gain deeper understanding of the differences in memory B cell responses between

216   individuals who had either non-severe or severe COVID-19, we combined the acquired flow

217   cytometry data for all 19 markers (**Table S2**) of all individuals and plotted a composite image

218   using Uniform Manifold Approximation Projection (UMAP). UMAP clusters cells in a 2D plot

219   based on similarity in phenotype and therefore provides meaningful organization of cell subsets.

220   For each recovered COVID-19 patient, we took a random sample of cells (n = 10,000) and

221   projected the spike-specific antigen-experienced B cells onto the composite UMAP (**Figure 4A**).

222   We also plotted contours for various B cell subsets to visualize their location within the UMAP

223   (**Figure 4B,** see **Figure S3** for heatmaps of all individual markers overlaid on the composite

224   UMAP). The composite image shows differences in the location of spike-specific B cells,

225   predominantly among IgG$^+$ B cells (**Figure 4A, B**). The large majority of IgG$^+$ B cells are

226   memory B cells, but a small fraction of these cells are DN1 B cells that are thought to contribute

227   to a functional immune response and were therefore included in a phenotypic analysis of spike-

228   specific IgG$^+$ B cells.

229

230   Irrespective of disease severity, spike-specific IgG$^+$ B cells expressed increased levels of

231   activation markers CD80, Ki-67, and CD95 (**Figure 4C**) compared to all IgG$^+$ B cells, with no

232   differences between the two groups. In contrast, spike-specific IgG$^+$ B cells after non-severe

233   disease showed an increase in the expression of the transcription factor T-bet that was not seen

234   after severe disease (**Figure 4D**). A median of 28% of spike-specific IgG$^+$ B cells in individuals

235   who experienced non-severe disease expressed T-bet, which has been associated with strong

236   anti-viral immunity (41). Conversely, T-bet was expressed in only about 10% of spike-specific

237   IgG$^+$ memory B cells in individuals who recovered from severe disease (**Figure 4D**). T-bet$^+$ cells

238   often have a distinct cell surface marker profile, including expression of CD11c and FcRL5 and

239   the absence of CD21 (25, 26, 28) . Indeed, in addition to T-bet, the percentage of both FcRL5$^+$

240   and CD11c$^+$ spike-specific IgG$^+$ memory B cells was increased among spike-specific IgG$^+$ B

241   cells in patients who recovered from non-severe COVID-19 as compared to all IgG$^+$ B cells in

242   these patients (**Figure 4D**), while these differences were not seen in individuals who recovered

243   from severe COVID-19. Conversely, a lower percentage of CD21$^+$ spike-specific IgG$^+$ B cells

244   was observed after non-severe disease but not after severe disease (**Figure 4D**). To confirm

245   that the measurement of T-bet, FcRL5, CD11c, and CD21 expression was robust between

246   experiments, we processed and analyzed technical replicates for samples from one non-severe

247   and one severe case on different days, and observed almost perfect correlation between the

248   replicates (Spearman r = 0.99, P = 0.0002, **Figure S4**). We then analyzed the combinatorial

249   expression of these markers by combining spike-specific IgG$^+$ T-bet$^+$ B cells from all donors and

250   plotting contour plots depicting the expression of FcRL5, CD11c, CD21, CD27, CXCR3, and

251   CXCR5 (**Figure 5**). This revealed four subpopulations of T-bet$^+$ IgG$^+$ B cells, of which cells

252   expressing FcRL5, CD11c, CD27 and CXCR3, and lacking CD21 and CXCR5 (type I; activated

253   switched memory B cells) were most abundant in both non-severe and severe cases (**Figure 5**).

254   This phenotype has previously been observed in activated B cells after influenza virus

255   vaccination and is thought to delineate a B cell subset associated with long-lived humoral

256   immunity (26, 28, 41). Collectively, the higher prevalence of spike-specific B cells that express

257   markers associated with durable immunity in individuals who recovered from non-severe

258   COVID-19 than in those who experienced severe disease suggests that disease severity

259   influences the quality of the B cell response.

260

261   **SARS-CoV-2 spike-specific memory B cells return to a resting phenotype with baseline**

262   **levels of T-bet expression five months post-symptom onset**

263   Activated T-bet$^+$ B cell subsets have been shown to expand and contract rapidly following

264   influenza virus vaccination, peaking between 14 and 28 days post-vaccination and returning to

265   baseline levels after three months (25). In addition, it has been shown that the memory B cell

266   response continues to mature up to one year following SARS-CoV-2 infection, giving rise to B

267   cell clones with higher levels of somatic hypermutation and resulting in increases in antigen-

268   binding affinity and ability to neutralize the virus (7, 19, 20). To evaluate the early dynamics of T-

269   bet$^+$ spike-specific B cells and continued development of the phenotype of memory B cells in

270   parallel with ongoing selection and maturation, we analyzed additional blood samples from

271   recovered COVID-19 patients with non-severe disease collected at an earlier time point

272   (median, 19 days post-symptom onset) (T1, **Figure 1**) and at a follow-up visit five months post-

273   symptom onset (T3, **Figure 1**). Unfortunately, we were unable to recruit any individuals who had

274   experienced severe disease for a follow-up visit at five months post-symptom onset. In addition,

275   at the earlier time point, most individuals with severe disease were still hospitalized (**Figure 1**).

276   We therefore limited this analysis to individuals who recovered from non-severe COVID-19.

277

278   The percentages of total naïve, unswitched memory, resting switched memory, activated

279   switched memory, and double negative B cell subsets among total B cells did not differ between

280   the two time points (**Figure S5**). However, the phenotype of spike-specific B cells changed

281   considerably between the two early time points and five months post-symptom onset (**Figure**

282   **6A, Figure S6**), as described in further detail below. Similar to what has been reported by Dan

283   *et al.* and Sokal *et al.* (4, 8), the percentage of spike-specific B cells among antigen-experienced

284   B cells remained relatively stable at five months post-symptom onset (**Figure 6B**). In addition,

285   the reactivity against RBD among these spike-specific B cells increased between 2 – 3 weeks

286   and 4 – 5 weeks post-symptom onset, but did not change at the 5-month time point (**Figure 6C**).

287   The larger proportion of non-RBD-specific B cells early in infection may be the result of recall

288   responses of pre-existing memory B cells that are cross-reactive with other coronaviruses.

289

290   The percentage of antigen-experienced spike-specific B cells with an unswitched memory B cell

291   phenotype was reduced at the 5-month time point (**Figure 6D**). The percentage of spike-specific

292   activated switched memory B cells drastically decreased over time, accompanied by an

293   increase in resting memory B cells (**Figure 6E**). Among switched memory B cells, the

294   percentage of IgM^+ and IgA^+ memory B cells declined and the proportion of IgG^+ memory B cells

295   increased at five months post-symptom onset (**Figure 6F**). In line with the decrease of IgM^+

296   memory B cells, the anti-spike and anti-RBD plasma IgM responses were lost almost completely

297   at five months post-symptom onset. Plasma IgG titers against the spike protein remained stable,

298   whereas plasma IgG titers against RBD showed a modest decrease (**Figure 6G**). These results

12

299   indicate that both the unswitched plasma cell and memory B cell response against the spike

300   protein are short-lived, while the class-switched IgG$^+$ response is more durable, as has been

301   reported by others (4, 8).

302

303   Both the decrease of unswitched memory B cells and the change from an activated to a resting

304   switched memory B cell phenotype can be seen in composite UMAPs of the three time points

305   (**Figure 7A-B**). In line with the return to a resting memory B cell phenotype, expression of

306   CD80, Ki-67, and CD95 was decreased at 20 – 23 weeks post-symptom onset as compared the

307   two earlier time points (**Figure 7C**). The percentage of CD80$^+$ spike-specific IgG$^+$ B cells at 20 –

308   23 weeks post-symptom onset still showed an increase over baseline levels (P = 0.016,

309   Wilcoxon signed rank test), while expression of Ki-67 and CD95 had returned to levels seen in

310   non-spike-specific IgG$^+$ B cells (**Figure 7C, Figure S7**). The expression of T-bet was higher at 2

311   – 3 weeks post-symptom onset than at 4 – 5 weeks post-symptom onset (median, 58% and

312   28%, respectively), although this difference was not statistically significant, and decreased

313   further to baseline levels (~ 10%) at 20 – 23 weeks post-symptom onset (**Figure 7D,E**). Similar

314   dynamics were observed for FcRL5 and CD11c, while CD21 expression increased significantly

315   over time (**Figure 7E**). The percentage of type I T-bet$^+$ spike-specific IgG$^+$ B cells (activated

316   switched memory B cells) that dominated the early response decreased dramatically over time

317   (**Figure 7D**). Instead, the T-bet$^+$ spike-specific IgG$^+$ B cells present at five months post-symptom

318   onset were mainly type II (FcRL5$^+$ CD11c$^+$ CD21$^-$ CD27$^-$, DN2 B cells) and type IV (FcRL5$^-$

319   CD11c$^-$ CD21$^+$ CD27$^+$, resting switched memory B cells) subsets, making up ~35% and ~40% of

320   T-bet$^+$ spike-specific IgG$^+$ B cells, respectively. These results suggest that the memory B cell

321   response continues to evolve until at least five months after infection. In addition, the decrease

322   of T-bet$^+$ spike-specific B cells in the circulation over the course of five months post-symptom

323   onset suggests that their abundant presence in the blood may signify recent exposure.

324

325 **DISCUSSION**

326 In the current COVID-19 pandemic, an important question that has only partially been answered

327 is whether SARS-CoV-2 infection elicits durable immunity. Assessments of B cell responses up

328 to one year post-infection suggest that both neutralizing antibodies and memory B cells against

329 the SARS-CoV-2 spike protein remain detectable in the circulation of most recovered COVID-19

330 patients and are stable or decay slowly at this time point. In this study, we aimed to better

331 understand the memory B cell response and to determine whether the severity of COVID-19

332 disease course influences the development of B cell responses. Using high-parameter spectral

333 flow cytometry, we analyzed the phenotype of B cells reactive with both non-RBD and RBD

334 epitopes on the spike protein shortly after recovery and approximately five months post-

335 symptom onset.

336

337 Our study consisted of a relatively small number of individuals but recapitulated many of the

338 observations reported from much larger cohorts, including the frequency of spike-specific

339 memory B cells after infection and the fraction of spike-specific B cells that recognizes RBD

340 epitopes. We also confirmed the loss of IgM^+ and IgA^+ spike-specific memory B cells and anti-

341 spike and anti-RBD plasma IgM, as well as maintenance of IgG^+ spike-specific memory B cells

342 and anti-spike plasma IgG five months post-symptom onset (4, 17). This gives us confidence in

343 the validity of several new observations that we discuss in more detail below.

344

345 The most striking result from this study is the higher percentage of spike-specific IgG^+ B cells

346 that express the transcription factor T-bet in individuals who recovered from non-severe disease

347 as compared to those who recovered from severe disease. Previously, it was observed that a

348 higher percentage of total $CD19^+$ $T\text{-}bet^+$ IgG_1^+ B cells was associated with shorter symptom

349 duration (42). Here, we determined that this association predominantly involves SARS-CoV-2

350 antigen-specific B cells, suggesting implications for the development of B cell memory. The

14

351   expression of T-bet, in parallel with a surface marker profile that includes the presence of FcRL5

352   and CD11c and the absence of CD21, has previously been reported on activated B cells shortly

353   after vaccination and infection, and is associated with long-lived humoral immunity (26, 28, 41).

354   Here, we observed that an increased percentage of spike-specific B cells showed this activated

355   phenotype shortly after recovery from non-severe COVID-19, but not after severe COVID-19.

356   Ogega *et al*. reported higher FcRL5 expression on RBD-specific class-switched memory B cells

357   after non-severe COVID-19 (non-hospitalized patients) than after severe disease (hospitalized

358   patients) (29), findings that are in agreement with our results. In addition, higher levels of

359   somatic hypermutation were observed in IgG$^+$ memory B cells following non-severe COVID-19

360   than severe disease (43), while patients who died from COVID-19 showed an absence of

361   germinal centers and a delay in the development of neutralizing antibodies (24, 44). Collectively,

362   these data are indicative of functional development of B cell immunity with germinal center

363   responses in patients with non-severe disease, as compared to a more dysfunctional B cell

364   response in severe disease cases.

365

366   T-bet expression in B cells can be induced by interferon gamma (IFNγ) signaling through the

367   IFNγ receptor (45, 46). IFNγ plays an important role in the immune response against viral

368   infections. Although many contradictory findings have been reported about the role of INFγ in

369   SARS-CoV-2 infection, the induction of INFγ early in infection seems important in the control of

370   viral replication [summarized in (47)]. Indeed, low IFNγ and low induction of interferon-

371   stimulated genes contribute to the development of COVID-19 (48). Failure to control viral load

372   leads to the induction of a hyper-inflammatory response later in disease, in parallel with

373   persistent high levels of IFNγ. However, these conditions may not promote the development of

374   T-bet$^+$ memory B cells. Instead, patients with severe disease show a strong extrafollicular B cell

375   response, resulting in an accumulation of DN2 B cells [(22)]. In our study, no difference was

376   observed in the percentage of DN2 B cells shortly after recovery between patients with either

377   non-severe or severe disease, suggesting that these DN2 B cells may be relatively short-lived.

378   Of note, DN2 cells typically also express T-bet (21), highlighting that the expression of this

379   transcription factor alone is not the determining factor in the development of either a functional

380   or pathogenic B cell response. The difference that we observed in the percentage of T-bet[+]

381   spike-specific IgG^{+} B cells between patients recovered from non-severe or severe COVID-19

382   could reflect these two developmental pathways of anti-viral immune responses.

383

384   In individuals who experienced non-severe COVID-19, T-bet[+] spike-specific IgG^{+} B cells almost

385   disappeared from the circulation five months post-symptom onset. This is in line with the

386   transient peak of activated memory B cells observed after influenza vaccination (25, 26). The

387   cell surface marker expression profile and dynamics of the T-bet^{+} B cells detected in this study

388   matches best with the AM2 subset of activated memory B cells defined by Andrews *et al*., which

389   peaked 14 days after influenza vaccination and had almost disappeared 90 days post-

390   vaccination (25). However, this does not necessarily mean that these cells are short-lived. It

391   was recently shown that the spleen harbors a population of resident T-bet[hi] memory B cells with

392   specificity to viral antigens (49). In addition, it has been reported that T-bet[hi] memory B cells

393   elicited in response to influenza virus vaccination rapidly differentiated into antibody-secreting

394   cells upon reactivation one year later (28). T-bet[+] memory B cells thus seem to contribute to

395   effective recall responses upon re-exposure, but may only be detectable in the circulation

396   shortly after infection. In this regard, it is important to point out that the timing of sampling can

397   strongly affect the frequency of transient B cell populations, and samples selected for

398   comparative analyses need to be carefully matched to account for rapid changes in the

399   abundance of activated B cell populations over time. For example, this may explain the

400   discrepancy between this study and the observation by Sokal *et al*. that T-bet expression in

401   spike-specific B cells was higher in individuals with severe COVID-19 than individual with non-

402   severe COVID-19 (8). In the Sokal *et al.* study, samples from severe cases were collected at an

16

403   earlier time point than those from non-severe cases (median, 18.8 days versus 35.5 days post-

404   symptom onset), which could have influenced these results (8).

405

406   Thus far, no differences have been observed in serum anti-spike antibody titers, *in vitro* serum

407   neutralizing activity, or percentages of spike-specific memory B cells between non-severe and

408   severe COVID-19 patients in the months after infection (18). It remains to be determined

409   whether the durability of B cell memory differs between individuals who experienced non-severe

410   or severe disease. We speculate that individuals who recovered from non-severe disease

411   develop a higher quality memory B cell response that may be longer-lived or may give rise to a

412   larger population of antibody-secreting cells upon re-exposure. An alternative interpretation of

413   the paucity of T-bet[+] spike-specific memory B cells in patients with severe disease could be that

414   a robust T-bet[+] B cell response protects against severe COVID-19. Although patients who died

415   from COVID-19 show defects in the development of B cell responses (24, 44), it is likely that the

416   expansion of a population of T-bet[+] spike-specific memory B cells is a consequence of the

417   immune environment during disease, not a factor contributing to survival. We believe these cells

418   are a sign of a balanced immune response that contributes to viral clearance through the

419   production of neutralizing antibodies and leads to the development of durable B cell memory,

420   but that T-bet[+] memory B cells do not play a direct role in protection against severe disease.

421

422   In conclusion, we have shown that the memory B cell response against SARS-CoV-2 spike

423   protein develops differently in patients with non-severe disease compared those with severe

424   disease, with more spike-specific B cells that express a B-cell marker profile associated with

425   durable immunity, characterized by expression of T-bet, FcRL5, and CD11c, and low expression

426   of CD21 in individuals who recovered from non-severe COVID-19. Although antibody titers or

427   percentage of spike-specific memory B cells up to one year are similar or higher in individuals

428   who recovered from severe disease as compared to non-severe cases (8, 18), the increased

17

429   percentage of B cells associated with long-lived immunity in non-severe COVID-19 patients may

430   have consequences for long-term immunity against SARS-CoV-2 re-infection or severity of the

431   resulting disease. T-bet[+] spike-specific B cells nearly disappeared from the circulation five

432   months post-symptom onset, consistent with loss of these cells from the periphery or migration

433   into tissues. These data aid in the understanding of naturally acquired B cell responses against

434   SARS-CoV-2 and help characterize the B cell populations that may be responsible for durable,

435   long-lived immunity.

436

437 **METHODS**

438 **Isolation of plasma and peripheral blood mononuclear cells**

439 Blood from recovered COVID-19 patients was processed within four hours of blood draw.

440 Plasma was separated from cells by centrifugation at 250 × g for 5 min at room temperature

441 (RT). Plasma was depleted of platelets by centrifugation at 2,000 × g for 15 min at 4°C and was

442 stored at -20°C. Peripheral blood mononuclear cells (PBMCs) were isolated from the cellular

443 fraction as described below. PBMCs used as negative controls were collected in 2018 and early

444 2019 by isolation from buffy coats (Interstate Blood Bank, Memphis, TN) obtained the day

445 following blood draw. Buffy coats were stored and shipped at room temperature (RT) and

446 processed immediately upon arrival. Cells were diluted approximately 4 × in PBS with 2 mM

447 EDTA. PBMCs were layered on Ficoll-Paque (GE Healthcare, cat. no. 17144002) and spun at

448 760 × g for 20 min at RT to pellet erythrocytes and separate leukocytes. The leukocytes were

449 then washed in PBS with 2 mM EDTA, centrifuged at 425 × g for 15 min at RT, followed by

450 centrifugation at 250 × g for 10 min at RT for all subsequent wash steps necessary to remove all

451 platelets, determined by cloudiness of the supernatant. Next, PBMCs were resuspended in cold

452 IMDM/GlutaMAX (Gibco, cat. no. 31980030) supplemented with 10% heat-inactivated, USA-

453 sourced, fetal bovine serum (FBS) and 5% cell culture grade DMSO, counted, and

454 cryopreserved in the liquid nitrogen vapor phase.

455

456 **Spike and RBD protein production and tetramer synthesis**

457 Recombinant SARS-CoV-2 HexaPro spike and RBD were produced from Addgene plasmid

458 #154754 (50) and BEI plasmid NR-52309, respectively, for use in ELISA experiments. DNA

459 plasmids were purified from DH5alpha Competent Cell (Zymo, cat. no. T3007) cultures using a

460 ZymoPURE II Plasmid Maxiprep (Zymo, cat. no. D4203). 25 µg plasmid was used to transfect

461 25 ml Expi293F (Thermo, cat. no. A14635) culture per manufacturer's instructions. Culture

462 supernatants were collected 5 days post-transfection. His-tagged S and RBD were purified

19

463   using HiTrap chelating high performance columns (Cytiva, cat. no. 17-0408-01) charged with

464   Ni^{2+}, washed with PBS (pH 7.2), and eluted with 0.3 M imidazole in PBS (pH

465   7.2). The imidazole was removed from the eluted protein buffer using a HiPrep desalting column

466   (Cytiva, cat. no. 17-5087-01). The protein was concentrated using a 30 kDa MWCO Amicon

467   ultra-15 centrifugal filter (Sigma, cat. no. UFC903024), and stored at -70°C. For the production

468   of biotinylated S and RBD protein used for the synthesis of antigen tetramers, Addgene plasmid

469   #154754 and BEI plasmid NR-52309 were altered to include a biotinylation site. The modified

470   plasmids have been deposited to Addgene: #166856 and #166857 for spike and RBD,

471   respectively. Cells were co-transfected with either plasmid #166856 or #166857 and a plasmid

472   encoding BirA ligase (Addgene #32408) at a 4:1 ratio (m/m). 100 mM D-biotin (Sigma, cat. no.

473   B4639) was added immediately post-transfection to a final concentration of 10 mM. Spike and

474   RBD tetramers were synthesized by incubating biotinylated protein with fluorophore-conjugated

475   streptavidin overnight at 4°C (streptavidin-PE, Tonbo, cat. no. 50-4317-U100, streptavidin-APC,

476   Tonbo, cat. no. 20-4317-U100, streptavidin-BV421, BioLegend, cat. no. 405226) at a molar ratio

477   of 5:1, respectively, to generate three individual tetramers: spike-PE, spike-APC, and RBD-

478   BV421.

479

480   **Protein gels**

481   As a quality control step, purified spike and RBD proteins were visualized on a polyacrylamide

482   gel (**Figure S8**). 800 ng of protein was loaded on a 4 – 12% Bis-Tris gel (Thermo, cat. no.

483   NP0321BOX) after it was mixed with 2× Laemmli loading buffer and incubated at 85°C for 5

484   min. The gel was run with MOPS running buffer (Thermo, cat. no. NP0001) at 200 V for 50 min

485   after which the proteins were stained using Imperial Protein Stain (Thermo, cat. no. PI24615)

486   per manufacturer's instructions.

487

488   **B cell isolation and staining**

20

489 Cryopreserved PBMCs were thawed in a water bath set at 37°C and immediately mixed with

490 pre-warmed thawing medium (IMDM/GlutaMAX supplemented with 10% heat inactivated FBS

491 and 0.01% Universal Nuclease (Thermo, cat. no. 88700). After brief centrifugation (250 × g, 5

492 min) at RT, the cell pellet was resuspended in warm thawing medium and viable cells were

493 counted using trypan blue on a Cellometer Mini (Nexcelom) automated cell counter. Next, the

494 PBMCs were pelleted (250 × g, 5 min, RT), resuspended in isolation buffer (PBS supplemented

495 with 2% heat inactivated FBS and 1 mM EDTA) at 50 million live cells/ml, and filtered through a

496 35 μm sterile filter cap (Corning, cat. no. 352235) to break apart any aggregated cells. B cells

497 were isolated using the EasySep Human B Cell Isolation Kit (StemCell, cat. no. 17954)

498 according to manufacturer's instructions. After washing with cold PBS (250 × g, 5 min, RT), the

499 isolated B cells were incubated with 1 μl Zombie UV Fixable Viability kit (Biolegend, cat. no.

500 423107) per 1 ml cell suspension for 30 min on ice. Cells were subsequently washed with cold

501 PBS with 1% bovine serum albumin (BSA), followed by an incubation at 4°C for 30 min with an

502 antigen tetramer cocktail (**Table S2**). Next, the cells were washed again with cold PBS with 1%

503 BSA and incubated at 4°C for 30 min with a B cell surface marker antibody cocktail (**Table S2**),

504 after which the cells were washed again with cold PBS with 1% BSA and resuspended in 1 ml

505 Transcription Factor Fix/Perm Concentrate (Tonbo, part of cat. no. TNB-0607-KIT) diluted with 3

506 parts Transcription Factor Fix/Perm Diluent (Tonbo) and incubated at 4°C for 1 hour. After the

507 incubation, the cells were washed twice with 3 ml of 1× Flow Cytometry Perm Buffer (Tonbo)

508 and resuspended in intracellular marker antibody cocktail (**Table S2**) diluted in 1× Flow

509 Cytometry Perm Buffer. After an incubation at 4°C for 30 min., the cells were washed twice with

510 3 ml 1× Flow Cytometry Perm Buffer and once with 3 ml cold PBS + 1% BSA. The cells were

511 then fixed by adding 4% formaldehyde at a 1:1 ratio to sample (v/v), washed with 3 ml cold PBS

512 + 1% BSA, and resuspended to 20 – 30 million cells/ml in PBS with 1% BSA, and filtered into a

513 FACS tube through a 35 μm sterile filter cap. Cells were analyzed by flow cytometry

514 immediately following fixation.

515

Flow cytometry analysis

517 B cells were analyzed on a Cytek Aurora spectral flow cytometer equipped with five lasers.

518 SpectroFlo QC Beads (Cytek, cat. no. SKU N7-97355) were run prior to each experiment for

519 performance tracking. Quality control and LJ tracking reports were used to ensure machine

520 performance and settings between different runs were comparable. B cells isolated from control

521 PBMCs collected pre-pandemic were used for the compensation of the live/dead stain and for

522 the unstained control. UltraComp eBeads (Thermo, cat. no. 01-2222-41) were used for

523 compensation of all other single stain fluorophores. FlowJo was used for gating and quantifying

524 cell frequencies. The cytometry analysis software OMIQ was used for the integration and

525 dimension reduction analysis. In short, Uniform Manifold Approximation and Projection (UMAPs)

526 where created by first pre-gating single/live/CD19$^+$/CD20$^+$/CD38^{lo} cells. Features used for

527 UMAP projection included mean fluorescence intensity of staining markers, excluding live/dead,

528 RBD, spike1, and spike2 with default parameters (neighbors = 15, metric = Euclidean, random

529 seed = 9889) and included all COVID-19 samples used in this study for initial projection.

530 Subsequently, files were subsampled to include an equal representation of cells from each

531 donor and concatenated within each group. For the projection of B cell subsets, Ig isotypes, and

532 antigen-specific B cells onto the UMAP, gates were manually set to identify populations of

533 interest using two-dimensional displays, which were then overlaid onto the UMAP projection.

534

Detection of spike protein and receptor binding domain using an enzyme-linked

immunosorbent assay

537 96-well plates (Corning, cat. no. 07-200-721) were coated with 50 μl of SARS-CoV-2 spike or

538 RBD at a concentration of 2 μg per ml in PBS and incubated overnight at 4ºC. An additional

539 plate was coated with goat anti-human IgG (Sigma, cat. no. I2136-1ML) at 4 μg/ml and IgM

540 (Sigma, cat. no. I1636-2ML) at 8 μg/ml, and served as a positive control. Plates were washed

541   twice using a gentle stream of deionized water from a faucet and subsequently incubated with

542   200 μl blocking buffer (PBS with 0.01% Tween-20 (Fisher, cat. no. BP337-100) and 3% non-fat

543   dry milk (SACO)) for 1 hour at RT. Three-fold serial dilutions of 20 μg/ml human IgG or IgM

544   were prepared in dilution buffer (PBS with 0.01% Tween-20 and 1% non-fat dry milk) and were

545   added to the IgG or IgM-coated and blocked plates in 100 μl total volume. Plasma samples

546   were heat inactivated prior to handling by incubating at 56°C for 30 min. Plasma samples were

547   then diluted in dilution buffer starting at a 1:50 dilution, with an additional 7 two-fold serial

548   dilutions. The diluted plasma samples, 27 from convalescent patients exposed to SARS-CoV-2

549   and 1 from a non-infected human control, were added to the plates in a total volume of 200 μl.

550   After a two-hour incubation at RT, the plates were washed once with 150 μl of PBST by

551   removing the samples and adding PBST by pipetting and subsequently washed 6 times using a

552   gentle stream of deionized water from a faucet. Next, 100 μl anti-human IgG or IgM -

553   horseradish peroxidase (HRP) conjugates (BioLegend), diluted 1:2500 and 1:5000 in dilution

554   buffer, respectively, was added and the plates were incubated for 1 hour at RT. After four

555   subsequent washes with deionized water 100 μl TMB (Thermo, cat. no. PI34024) was added

556   and the plates were incubated in the dark at RT. The oxidation of TMB was stopped by adding

557   100 μl 0.18 M H_2SO_4 when the wells containing the most diluted IgG/IgM standard started to

558   color. The absorbance was measured at 450 nm using a Synergy H4 Hybrid Plate Reader

559   (BioTek). The average background signal of wells incubated without plasma was subtracted

560   from the absorbance values for each sample. All plasma samples were measured in duplicate

561   and the average absorbance reading was used to calculate the area under the curve using

562   GraphPad 9.

563

564   **Statistics**

565   Statistical analyses were performed in GraphPad 9. Differences between two groups were

566   evaluated using a Mann-Whitney U test. Differences in the expression of intracellular and cell

567   surface markers were tested using a Kruskal-Wallis test, followed by comparisons between

568   selected pairs of groups using Dunn's post-hoc test, corrected for multiple comparisons. Non-

569   parametric tests were used because the limited sample size did not allow for reliable evaluation

570   of normal distribution and homoscedasticity.

571

572   **Study approval**

573   Samples and associated clinical data used in this study were received de-identified from the

574   University of Texas Health San Antonio COVID-19 Repository. This repository was reviewed

575   and approved by the University of Texas Health Science Center at San Antonio Institutional

576   Review Board. All study participants provided written informed consent prior to specimen

577   collection for the repository to include collection of associated clinical information and use of left-

578   over clinical specimens for research. The COVID-19 Repository utilizes an honest broker

579   system to maintain participant confidentiality and release of de-identified data or specimens to

580   recipient investigators.

581 **AUTHOR CONTRIBUTIONS**

582 EMB secured funding for the study. RAR and EMB conceived the research question and

583 designed the study. RAR isolated plasma and PBMCs, and acquired and analyzed flow

584 cytometry data. KC performed and analyzed ELISAs. RAR, SB, and SJG produced S protein

585 and RBD, which were purified by AMC. GC, RET, and TFP provided clinical samples and data.

586 RG provided critical feedback on the manuscript. RAR, SB, and EMB wrote the manuscript with

587 input from all other co-authors.

598

599

REFERENCES

1. WHO Coronavirus Dashboard. Accessed September 17, 2021.

2. Goel RR, Apostolidis SA, Painter MM, Mathew D, Pattekar A, Kuthuru O, et al. Distinct antibody and memory B cell responses in SARS-CoV-2 naive and recovered individuals following mRNA vaccination. *Sci Immunol.* 2021;6(58).

3. Greaney AJ, Loes AN, Gentles LE, Crawford KHD, Starr TN, Malone KD, et al. Antibodies elicited by mRNA-1273 vaccination bind more broadly to the receptor binding domain than do those from SARS-CoV-2 infection. *Sci Transl Med.* 2021;13(600).

4. Dan JM, Mateus J, Kato Y, Hastie KM, Yu ED, Faliti CE, et al. Immunological memory to SARS-CoV-2 assessed for up to 8 months after infection. *Science.* 2021;371(6529).

5. Turner JS, Kim W, Kalaidina E, Goss CW, Rauseo AM, Schmitz AJ, et al. SARS-CoV-2 infection induces long-lived bone marrow plasma cells in humans. *Nature.* 2021;595(7867):421-5.

6. Hartley GE, Edwards ESJ, Aui PM, Varese N, Stojanovic S, McMahon J, et al. Rapid generation of durable B cell memory to SARS-CoV-2 spike and nucleocapsid proteins in COVID-19 and convalescence. *Sci Immunol.* 2020;5(54).

7. Wang Z, Muecksch F, Schaefer-Babajew D, Finkin S, Viant C, Gaebler C, et al. Naturally enhanced neutralizing breadth against SARS-CoV-2 one year after infection. *Nature.* 2021;595(7867):426-31.

8. Sokal A, Chappert P, Barba-Spaeth G, Roeser A, Fourati S, Azzaoui I, et al. Maturation and persistence of the anti-SARS-CoV-2 memory B cell response. *Cell.* 2021;184(5):1201-13 e14.

9. Lumley SF, O'Donnell D, Stoesser NE, Matthews PC, Howarth A, Hatch SB, et al. Antibody Status and Incidence of SARS-CoV-2 Infection in Health Care Workers. *N Engl J Med.* 2021;384(6):533-40.

10. Abu-Raddad LJ, Chemaitelly H, Coyle P, Malek JA, Ahmed AA, Mohamoud YA, et al. SARS-CoV-2 antibody-positivity protects against reinfection for at least seven months with 95% efficacy. *EClinicalMedicine.* 2021;35:100861.

11. Hansen CH, Michlmayr D, Gubbels SM, Molbak K, and Ethelberg S. Assessment of protection against reinfection with SARS-CoV-2 among 4 million PCR-tested individuals in Denmark in 2020: a population-level observational study. *Lancet.* 2021;397(10280):1204-12.

12. Grifoni A, Weiskopf D, Ramirez SI, Mateus J, Dan JM, Moderbacher CR, et al. Targets of T Cell Responses to SARS-CoV-2 Coronavirus in Humans with COVID-19 Disease and Unexposed Individuals. *Cell.* 2020;181(7):1489-501 e15.

13. Rodda LB, Netland J, Shehata L, Pruner KB, Morawski PA, Thouvenel CD, et al. Functional SARS-CoV-2-Specific Immune Memory Persists after Mild COVID-19. *Cell.* 2021;184(1):169-83 e17.

14. Roltgen K, and Boyd SD. Antibody and B cell responses to SARS-CoV-2 infection and vaccination. *Cell Host Microbe.* 2021;29(7):1063-75.

15. Seow J, Graham C, Merrick B, Acors S, Pickering S, Steel KJA, et al. Longitudinal observation and decline of neutralizing antibody responses in the three months following SARS-CoV-2 infection in humans. *Nat Microbiol.* 2020;5(12):1598-607.

643 16. Legros V, Denolly S, Vogrig M, Boson B, Siret E, Rigaill J, et al. A longitudinal study of
644   SARS-CoV-2-infected patients reveals a high correlation between neutralizing antibodies
645   and COVID-19 severity. *Cell Mol Immunol.* 2021;18(2):318-27.

646 17. Cohen KW, Linderman SL, Moodie Z, Czartoski J, Lai L, Mantus G, et al. Longitudinal
647   analysis shows durable and broad immune memory after SARS-CoV-2 infection with
648   persisting antibody responses and memory B and T cells. *Cell Rep Med.*
649   2021;2(7):100354.

650 18. Sandberg JT, Varnaite R, Christ W, Chen P, Muvva JR, Maleki KT, et al. SARS-CoV-2-
651   specific humoral and cellular immunity persists through 9 months irrespective of COVID-19
652   severity at hospitalisation. *Clin Transl Immunology.* 2021;10(7):e1306.

653 19. Sakharkar M, Rappazzo CG, Wieland-Alter WF, Hsieh CL, Wrapp D, Esterman ES, et al.
654   Prolonged evolution of the human B cell response to SARS-CoV-2 infection. *Sci Immunol.*
655   2021;6(56).

656 20. Muecksch F, Weisblum Y, Barnes CO, Schmidt F, Schaefer-Babajew D, Wang Z, et al.
657   Affinity maturation of SARS-CoV-2 neutralizing antibodies confers potency, breadth, and
658   resilience to viral escape mutations. *Immunity.* 2021;54(8):1853-68 e7.

659 21. Jenks SA, Cashman KS, Zumaquero E, Marigorta UM, Patel AV, Wang X, et al. Distinct
660   Effector B Cells Induced by Unregulated Toll-like Receptor 7 Contribute to Pathogenic
661   Responses in Systemic Lupus Erythematosus. *Immunity.* 2018;49(4):725-39 e6.

662 22. Woodruff MC, Ramonell RP, Nguyen DC, Cashman KS, Saini AS, Haddad NS, et al.
663   Extrafollicular B cell responses correlate with neutralizing antibodies and morbidity in
664   COVID-19. *Nat Immunol.* 2020;21(12):1506-16.

665 23. Stewart A, Ng JC, Wallis G, Tsioligka V, Fraternali F, and Dunn-Walters DK. Single-Cell
666   Transcriptomic Analyses Define Distinct Peripheral B Cell Subsets and Discrete
667   Development Pathways. *Front Immunol.* 2021;12:602539.

668 24. Kaneko N, Kuo HH, Boucau J, Farmer JR, Allard-Chamard H, Mahajan VS, et al. Loss of
669   Bcl-6-Expressing T Follicular Helper Cells and Germinal Centers in COVID-19. *Cell.*
670   2020;183(1):143-57 e13.

671 25. Andrews SF, Chambers MJ, Schramm CA, Plyler J, Raab JE, Kanekiyo M, et al. Activation
672   Dynamics and Immunoglobulin Evolution of Pre-existing and Newly Generated Human
673   Memory B cell Responses to Influenza Hemagglutinin. *Immunity.* 2019;51(2):398-410 e5.

674 26. Lau D, Lan LY, Andrews SF, Henry C, Rojas KT, Neu KE, et al. Low CD21 expression
675   defines a population of recent germinal center graduates primed for plasma cell
676   differentiation. *Sci Immunol.* 2017;2(7).

677 27. Kim CC, Baccarella AM, Bayat A, Pepper M, and Fontana MF. FCRL5(+) Memory B Cells
678   Exhibit Robust Recall Responses. *Cell Rep.* 2019;27(5):1446-60 e4.

679 28. Nellore A, Zumaquero E, Scharer CD, King RG, Tipton CM, Fucile CF, et al. Influenza-
680   specific effector memory B cells predict long-lived antibody responses to vaccination in
681   humans. *bioRxiv.*

682 29. Ogega CO, Skinner NE, Blair PW, Park HS, Littlefield K, Ganesan A, et al. Durable SARS-
683   CoV-2 B cell immunity after mild or severe disease. *J Clin Invest.* 2021;131(7).

684 30. Beigel JH, Tomashek KM, Dodd LE, Mehta AK, Zingman BS, Kalil AC, et al. Remdesivir
685   for the Treatment of Covid-19 - Final Report. *N Engl J Med.* 2020;383(19):1813-26.

686 31. Kalil AC, Patterson TF, Mehta AK, Tomashek KM, Wolfe CR, Ghazaryan V, et al.
687   Baricitinib plus Remdesivir for Hospitalized Adults with Covid-19. *N Engl J Med.*
688   2021;384(9):795-807.

689 32. Lucas C, Wong P, Klein J, Castro TBR, Silva J, Sundaram M, et al. Longitudinal analyses
690   reveal immunological misfiring in severe COVID-19. *Nature.* 2020;584(7821):463-9.

691 33. Oliviero B, Varchetta S, Mele D, Mantovani S, Cerino A, Perotti CG, et al. Expansion of
692   atypical memory B cells is a prominent feature of COVID-19. *Cell Mol Immunol.*
693   2020;17(10):1101-3.

694 34. Barnes CO, Jette CA, Abernathy ME, Dam KA, Esswein SR, Gristick HB, et al. SARS-
695   CoV-2 neutralizing antibody structures inform therapeutic strategies. *Nature.*
696   2020;588(7839):682-7.

697 35. Voss WN, Hou YJ, Johnson NV, Delidakis G, Kim JE, Javanmardi K, et al. Prevalent,
698   protective, and convergent IgG recognition of SARS-CoV-2 non-RBD spike epitopes.
699   *Science.* 2021;372(6546):1108-12.

700 36. Jaimes JA, Andre NM, Chappie JS, Millet JK, and Whittaker GR. Phylogenetic Analysis
701   and Structural Modeling of SARS-CoV-2 Spike Protein Reveals an Evolutionary Distinct
702   and Proteolytically Sensitive Activation Loop. *J Mol Biol.* 2020;432(10):3309-25.

703 37. Nguyen-Contant P, Embong AK, Kanagaiah P, Chaves FA, Yang H, Branche AR, et al. S
704   Protein-Reactive IgG and Memory B Cell Production after Human SARS-CoV-2 Infection
705   Includes Broad Reactivity to the S2 Subunit. *mBio.* 2020;11(5).

706 38. Ng KW, Faulkner N, Cornish GH, Rosa A, Harvey R, Hussain S, et al. Preexisting and de
707   novo humoral immunity to SARS-CoV-2 in humans. *Science.* 2020;370(6522):1339-43.

708 39. Wang C, van Haperen R, Gutierrez-Alvarez J, Li W, Okba NMA, Albulescu I, et al. A
709   conserved immunogenic and vulnerable site on the coronavirus spike protein delineated
710   by cross-reactive monoclonal antibodies. *Nat Commun.* 2021;12(1):1715.

711 40. Song G, He WT, Callaghan S, Anzanello F, Huang D, Ricketts J, et al. Cross-reactive
712   serum and memory B-cell responses to spike protein in SARS-CoV-2 and endemic
713   coronavirus infection. *Nat Commun.* 2021;12(1):2938.

714 41. Knox JJ, Buggert M, Kardava L, Seaton KE, Eller MA, Canaday DH, et al. T-bet+ B cells
715   are induced by human viral infections and dominate the HIV gp140 response. *JCI Insight.*
716   2017;2(8).

717 42. Newell KL, Clemmer DC, Cox JB, Kayode YI, Zoccoli-Rodriguez V, Taylor HE, et al.
718   Switched and unswitched memory B cells detected during SARS-CoV-2 convalescence
719   correlate with limited symptom duration. *PLoS One.* 2021;16(1):e0244855.

720 43. Hoehn KB, Ramanathan P, Unterman A, Sumida TS, Asashima H, Hafler DA, et al.
721   Cutting Edge: Distinct B Cell Repertoires Characterize Patients with Mild and Severe
722   COVID-19. *J Immunol.* 2021.

723 44. Lucas C, Klein J, Sundaram ME, Liu F, Wong P, Silva J, et al. Delayed production of
724   neutralizing antibodies correlates with fatal COVID-19. *Nat Med.* 2021;27(7):1178-86.

725 45. Ambegaonkar AA, Nagata S, Pierce SK, and Sohn H. The Differentiation in vitro of Human
726   Tonsil B Cells With the Phenotypic and Functional Characteristics of T-bet+ Atypical
727   Memory B Cells in Malaria. *Front Immunol.* 2019;10:852.

728   46.   Zumaquero E, Stone SL, Scharer CD, Jenks SA, Nellore A, Mousseau B, et al. IFNgamma
729   induces epigenetic programming of human T-bet(hi) B cells and promotes TLR7/8 and IL-
730   21 induced differentiation. *Elife.* 2019;8.

731   47.   Mohseni Afshar Z, Babazadeh A, Hasanpour A, Barary M, Sayad B, Janbakhsh A, et al.
732   Dermatological manifestations associated with COVID-19: A comprehensive review of the
733   current knowledge. *J Med Virol.* 2021;93(10):5756-67.

734   48.   Blanco-Melo D, Nilsson-Payant BE, Liu WC, Uhl S, Hoagland D, Moller R, et al.
735   Imbalanced Host Response to SARS-CoV-2 Drives Development of COVID-19. *Cell.*
736   2020;181(5):1036-45 e9.

737   49.   Johnson JL, Rosenthal RL, Knox JJ, Myles A, Naradikian MS, Madej J, et al. The
738   Transcription Factor T-bet Resolves Memory B Cell Subsets with Distinct Tissue
739   Distributions and Antibody Specificities in Mice and Humans. *Immunity.* 2020;52(5):842-55
740   e6.

741   50.   Hsieh CL, Goldsmith JA, Schaub JM, DiVenere AM, Kuo HC, Javanmardi K, et al.
742   Structure-based design of prefusion-stabilized SARS-CoV-2 spikes. *Science.*
743   2020;369(6510):1501-5.

744
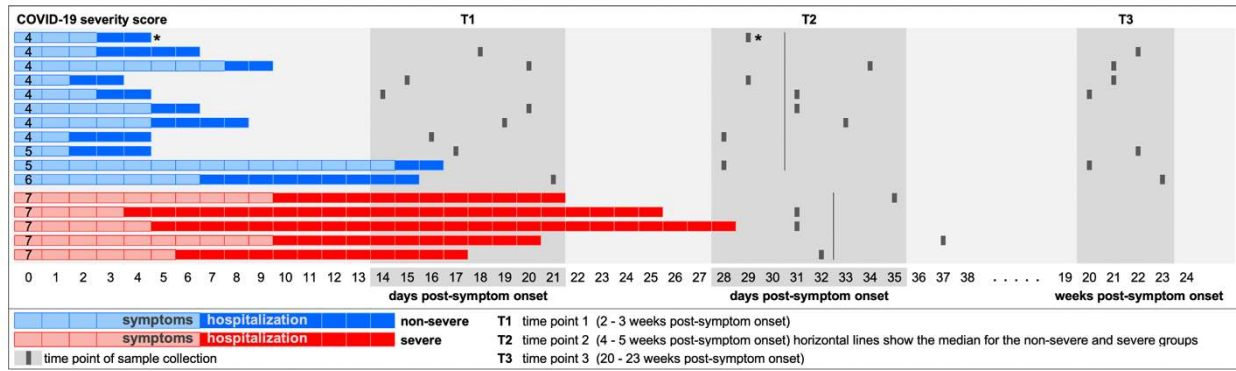
FIGURES

Figure 1: Timing of sample collection. Hospitalized COVID-19 patients were recruited for the study and sampled after hospital discharge. Samples from T2 were used for the comparison of B cell responses between individuals who recovered from non-severe and severe COVID-19 (**Figures 2 – 4**). All samples at T2 were collected 4 – 5 weeks post-symptom onset (PSO), with the exception of one severe donor who was sampled just after 5 weeks PSO (37 days). Longitudinal analysis of samples collected at T1 – T3 could only be performed for individuals who experienced non-severe disease, because the majority of severe patients were still hospitalized at T1 and we were unsuccessful in recruiting recovered severe patients for a follow-up blood draw at T3. The donor marked with * was included in the analysis of B cell subsets (**Figure 2**) and the percentage of spike-specific B cells (**Figure 3C**), but could not be included in all subsequent analyses because only a small number of spike-specific B cells (n = 6) was detected in this sample.

760

761
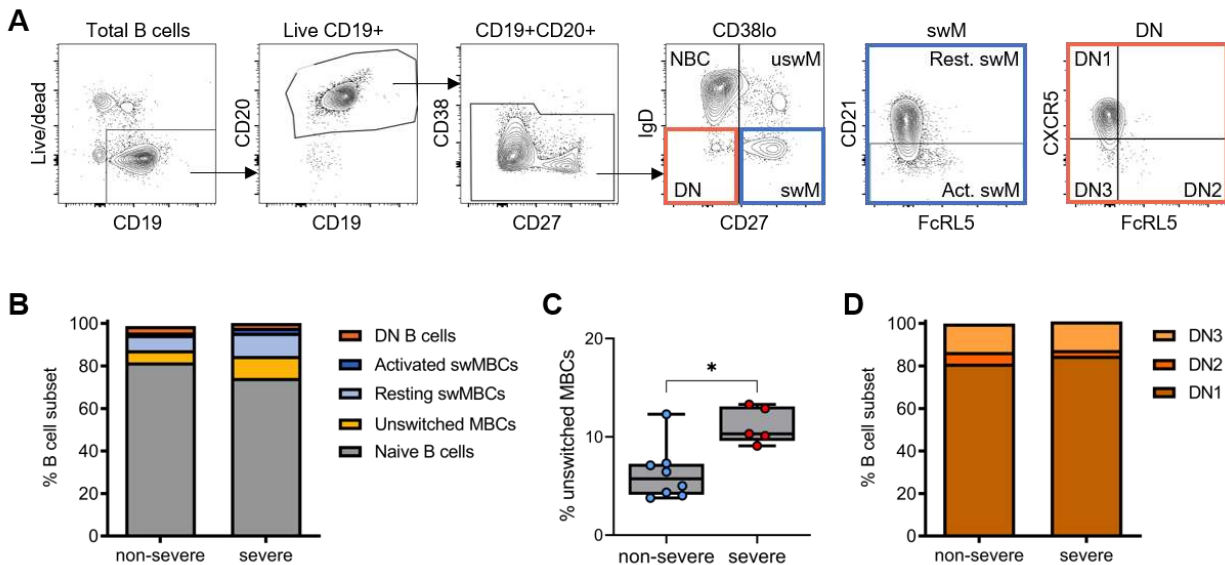
Figure 2: Distribution of major B cell subsets in recovered COVID-19 patients. A) Gating

strategy to obtain non-antibody-secreting B cells (CD38lo) that are further divided into naïve,

unswitched memory (uswM), switched memory (swM), and double negative (DN). SwM B cells

were divided into activated and resting populations based on the expression of CD21. DN cells

were divided into DN1 – 3 based on the expression of FcRL5 and CXCR5. **B)** Median

percentage of each B cell subset in samples from individuals who recovered from non-severe

COVID-19 and severe COVID-19. **C)** Percentage of unswitched memory B cells, which was

increased in individuals who recovered from severe disease as compared to those who had

non-severe COVID-19. **D)** Median proportions of the three different DN populations 1 month

after non-severe or severe disease. In panel B – D, results are shown for individuals who

recovered from non-severe COVID-19 (n = 8) and severe COVID-19 (n = 5). See **Figure S1** for

graphs with individual data points for the data shown in panels B and D. * P < 0.05
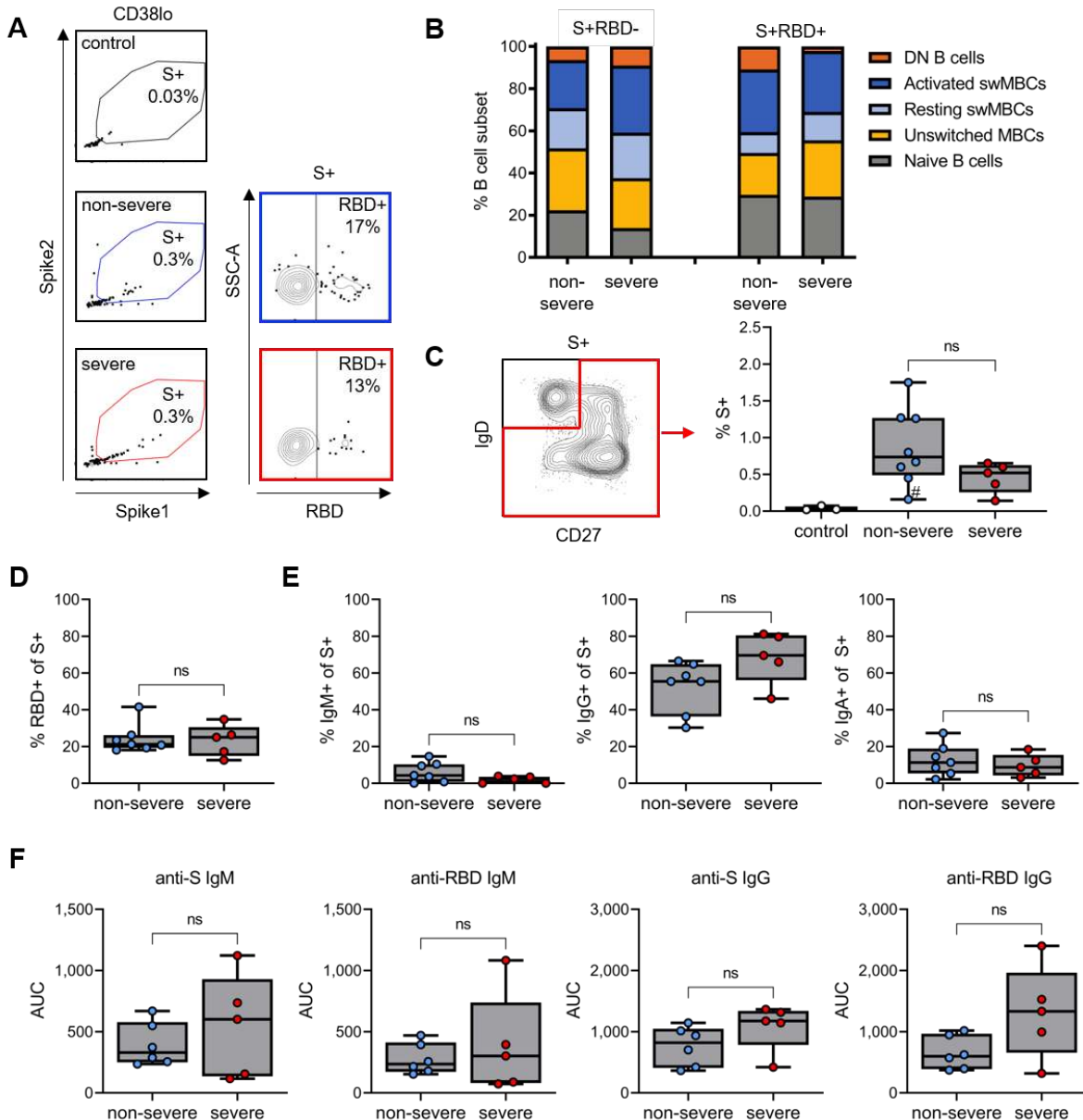
Figure 3: Detection of spike-specific and RBD-specific B cells and plasma antibody responses. A) Flow cytometry gating of spike-specific (S+) and RBD-specific (RBD+) B cells. **B)** Phenotype of non-RBD-specific (S+RBD-) and RBD-specific (S+RBD+) B cells, showing the median percentage among each group. Graphs with individual data points for each B cell subset are presented in **Figure S2**. **C)** Percentage of antigen-experienced spike-specific B cells in individuals who have never been exposed to SARS-CoV-2 (control) or who recovered from non-severe or severe disease. **D)** Percentage of spike-specific B cells that recognized RBD. **E)** Percentage of class-switched spike-specific B cells that express IgM (left), IgG (middle), or IgA (right). **F)** Plasma IgM (left) and IgG (right) titers against spike and RBD. Note that the range of the Y axes are different between IgM and IgG. In panel C, results are shown for individuals who recovered from non-severe COVID-19 (n = 8) and severe COVID-19 (n = 5). Only seven individuals with non-severe COVID-19 were included in panels B, D, and E, due to the low number of spike-specific B cells detected in the individual marked with # in panel C.

33
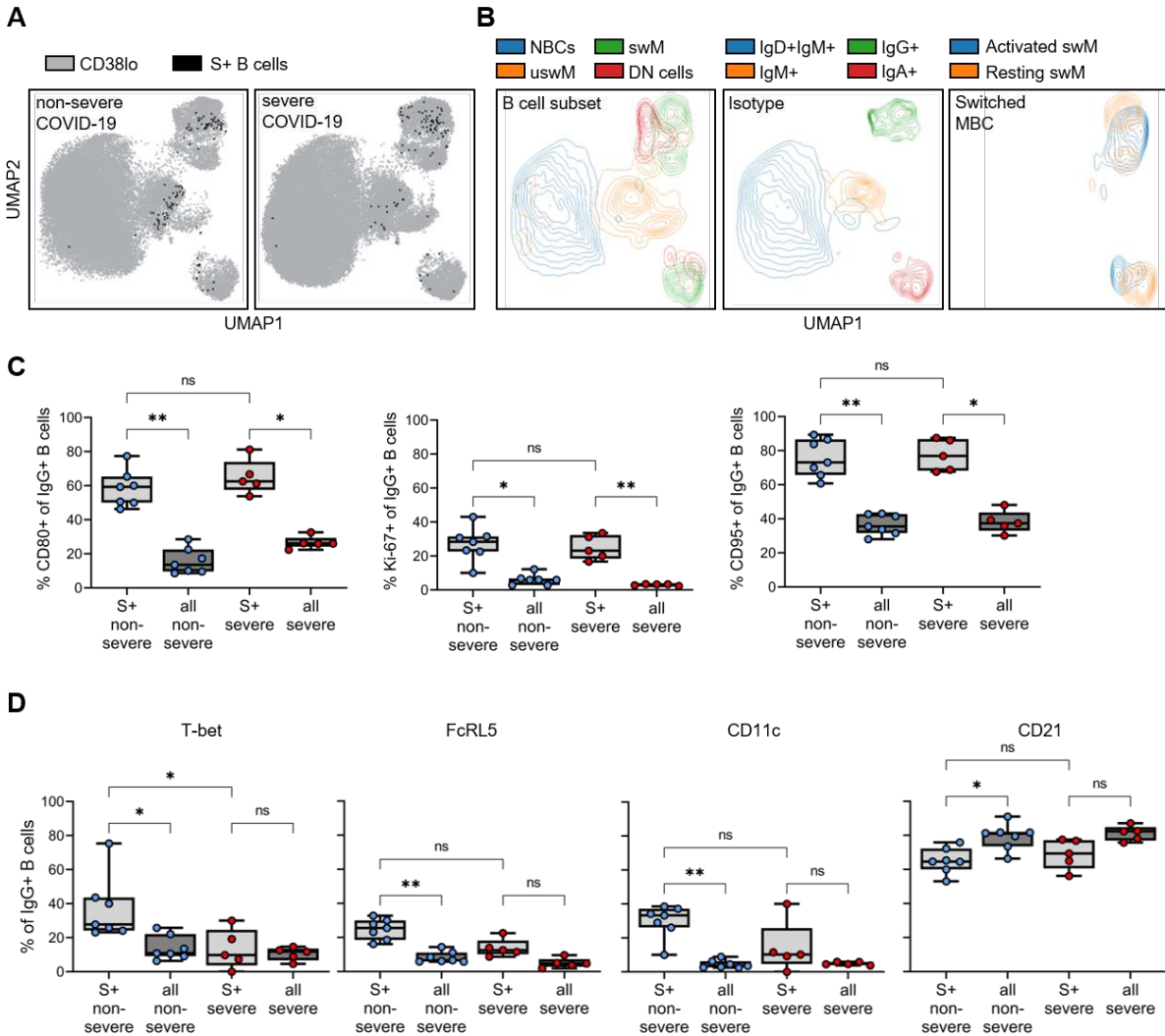
**Figure 4: Differences in the percentage spike-specific T-bet+ B cells between patients recovered from non-severe and severe COVID-19. A)** Composite UMAP showing the overlay of spike-specific B cells from individuals who recovered from non-severe (left) or severe (right) disease onto all B cells from that group. **B)** Overlay of major B cell subsets and isotypes onto the composite UMAP. **C)** Expression of CD80, Ki-67, and CD95 by spike-specific (S+) IgG+ B cells and all IgG+ B cells in individuals who experienced non-severe or severe COVID-19. **D)** Expression of T-bet, FcRL5, CD11c, and CD21 by spike-specific IgG+ B cells and all IgG+ B cells in individuals who experienced non-severe or severe COVID-19. Results are shown for seven individuals who recovered from non-severe COVID-19 and five patients who recovered from severe COVID-19. * P < 0.05; ** P < 0.01
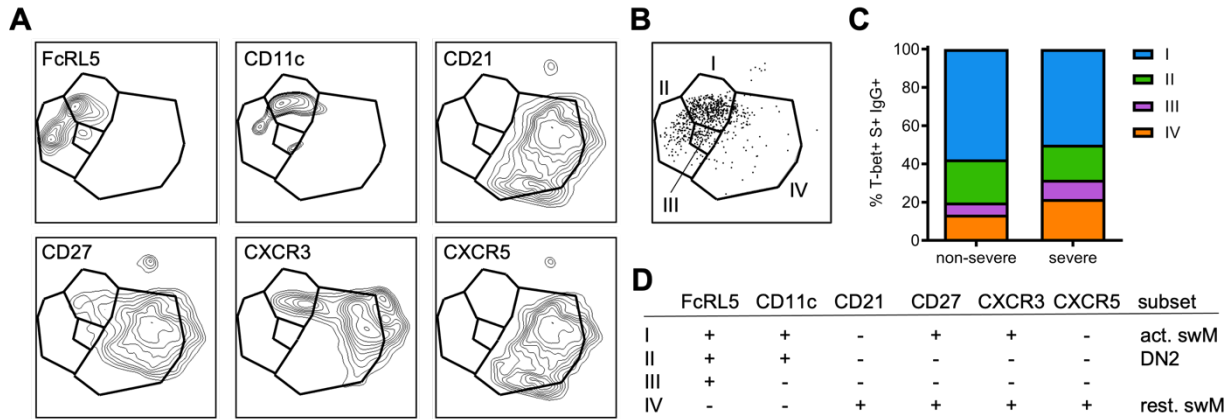
Figure 5: The phenotype of T-bet+ IgG+ spike-specific B cells. A) UMAPS showing the expression of individual markers in T-bet+ IgG+ spike-specific B cells. **B)** Gating of four populations of T-bet+ IgG+ B cells based on unique expression profiles of the markers shown in panel A. **C)** Distribution of the four T-bet+ IgG+ B cell population among individuals who recovered from non-severe (n = 7) and severe (n = 5) COVID-19. **D)** Summary of the phenotype of the four T-bet+ IgG+ B cell populations identified here and their classification into one of the major B cell subsets: activated switched memory (act. swM), DN2, or resting switched memory (rest. swM) B cells.

809
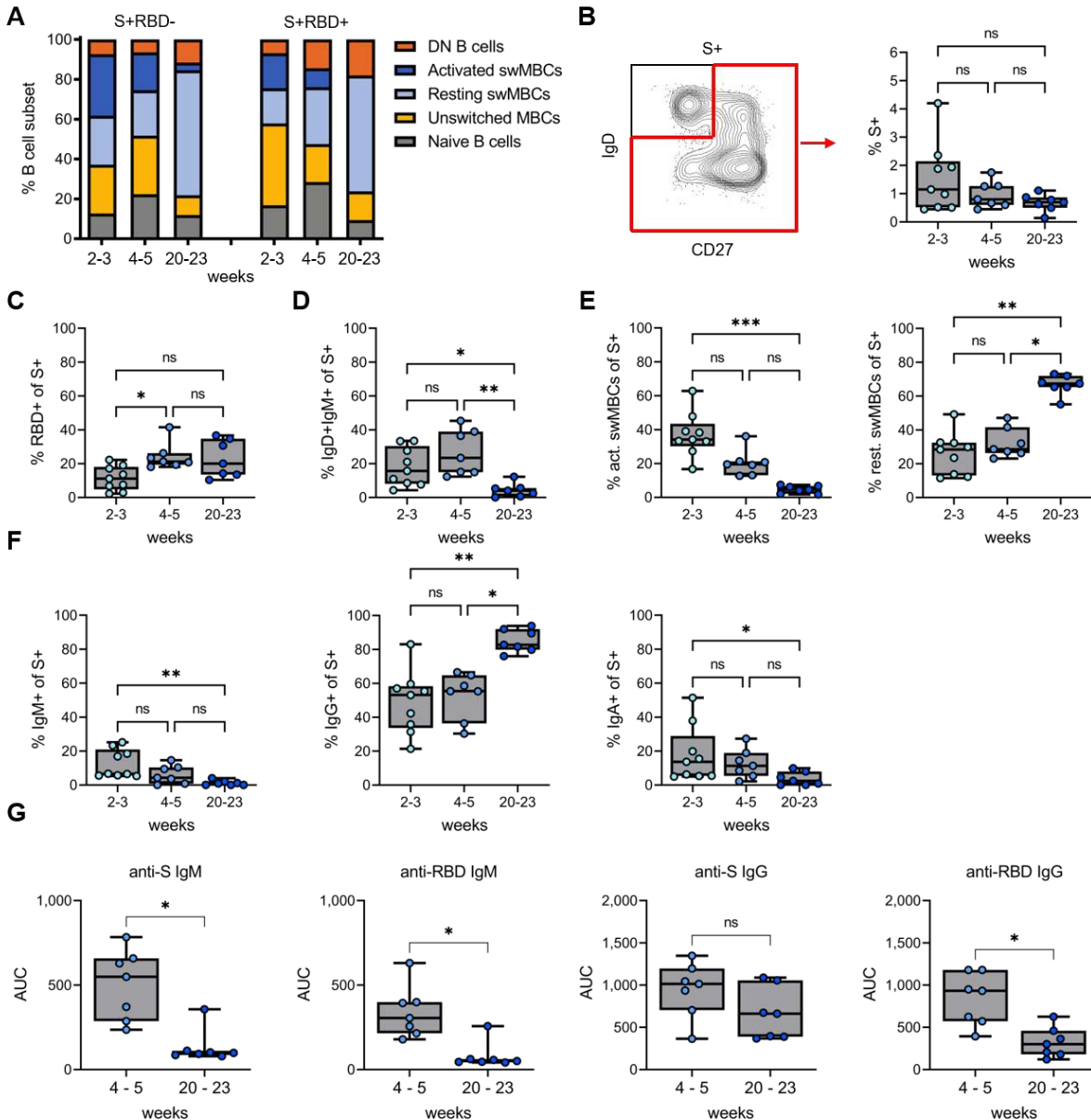
Figure 6: Change from activated to resting memory phenotype of IgG⁺ spike-specific B cells at five months post-symptom onset. A) Phenotype distribution of non-RBD-specific (S+RBD-) and RBD-specific (S+RBD+) B cells, showing the median percentage among each group. Graphs with individual data points for each B cell subset are presented in **Figure S6**. **B)** Percentage of antigen-experienced spike-specific B cells at 2 – 3, 4 – 5, and 20 – 23 weeks post-symptom onset. **C)** Percentage of S+RBD+ B cells among antigen-experienced spike-specific B cells. **D)** Percentage of unswitched memory B cells among antigen-experienced spike-specific B cells. **E)** Percentage of activated (left) and resting (right) switched memory B cells among antigen-experienced spike-specific B cells. **F)** Percentage of class-switched spike-specific B cells that express IgM (left), IgA (middle), or IgG (right). **G)** Plasma IgM (left) and IgG (right) titers against spike and RBD. In all panels, results are shown for samples collected 2 – 3 (n = 9), 4 – 5 (n = 7), and 20 – 23 (n = 7) weeks post-symptom onset. * P < 0.05; ** P < 0.01; *** P < 0.001

36
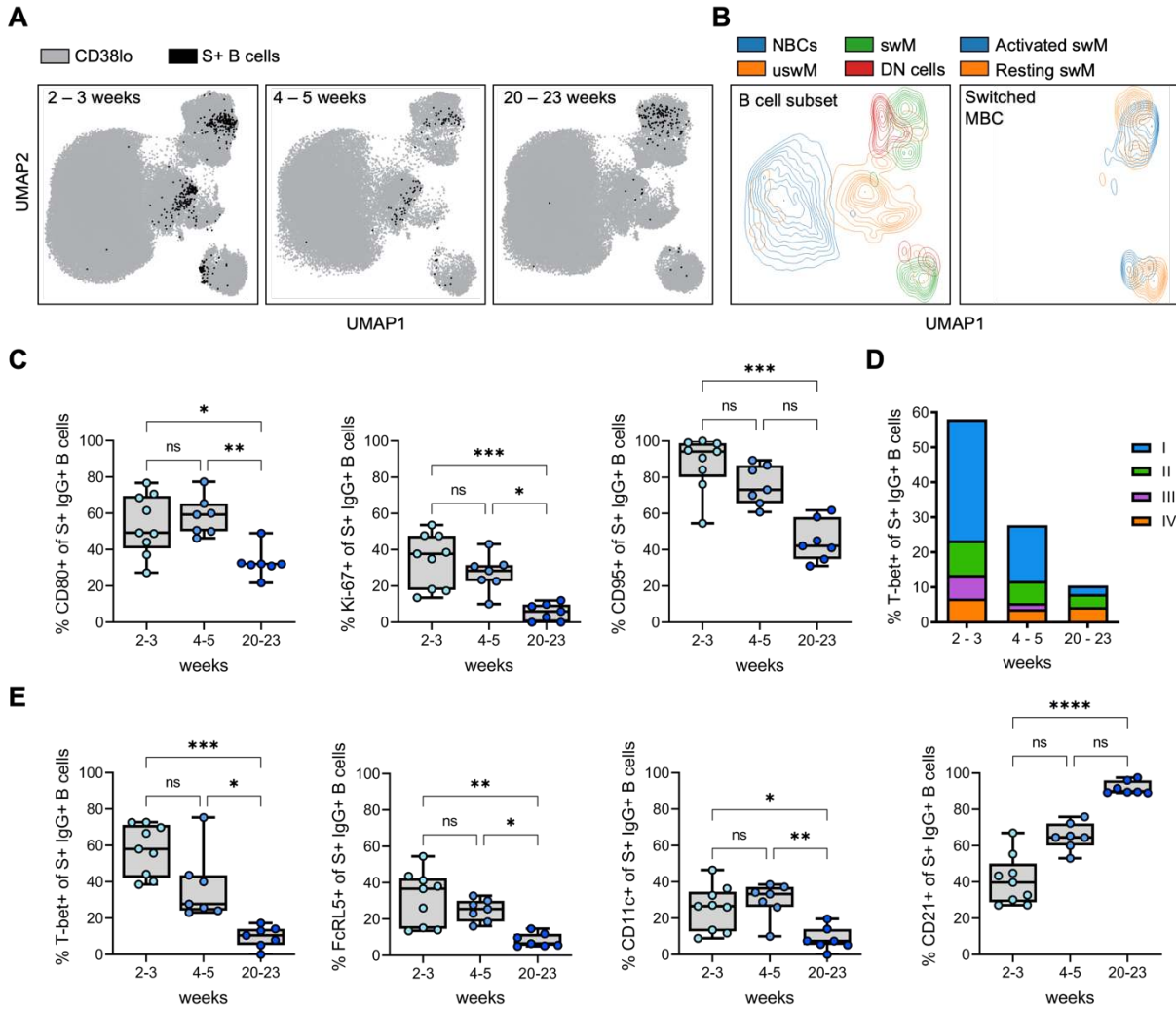
Figure 7: Longitudinal dynamics in the percentage of spike-specific B cells that express T-bet and various surface markers shortly after recovery and five months post-symptom onset. A) Composite UMAP showing the overlay of spike-specific B cells from individuals who recovered from non-severe COVID-19 at 2-3 (left), 4-5 (middle), and 20-23 (left) weeks post-symptom onset. **B)** Overlay of major B cell subsets and activated/resting switched memory B cells onto the composite UMAP. **C)** Expression of CD80, Ki-67, and CD95 by spike-specific (S+) IgG$^+$ B cells at the three time points. **D)** Distribution of the four T-bet$^+$ subsets (as defined in **Figure 5**) among spike-specific IgG$^+$ B cells at the three time points post-symptom onset. **E)** Expression of T-bet, FcRL5, CD11c, and CD21 by spike-specific IgG$^+$ B cells at the three time points post-symptom onset. In all graphs, results are shown for samples collected 2 – 3 (n = 9), 4 – 5 (n = 7), and 20 – 23 (n = 7) weeks post-symptom onset. * P < 0.05; ** P < 0.01; *** P < 0.001; **** P < 0.0001